Applied Physics Express

LETTER

Spin property improvement of boron vacancy defect in hexagonal boron nitride by thermal treatment

To cite this article: Tetta Suzuki *et al* 2023 *Appl. Phys. Express* **16** 032006

Applied Physics Express **16**, 032006 (2023) **LETTER**
https://doi.org/**10.35848/1882-0786/acc442**

Spin property improvement of boron vacancy defect in hexagonal boron nitride by thermal treatment

Tetta Suzuki[1,2], Yuichi Yamazaki[2*], Takashi Taniguchi[3], Kenji Watanabe[3], Yusuke Nishiya[4], Yu-ichiro Matsushita[2,4], Kazuya Harii[2], Yuta Masuyama[2], Yasuto Hijikata[1], and Takeshi Ohshima[2]

[1]*Saitama University, 225 Shimo-Okubo, Sakura-ku, Saitama 338-0825 Japan*
[2]*Quantum Materials and Applications Research Center, National Institutes for Quantum Science and Technology, 1233 Watanuki, Takasaki, Gunma 370-1292 Japan*
[3]*Research Center for Functional Materials, National Institute for Materials Science, 1-2-1 Sengen, Tsukuba, Ibaraki 305-0047, Japan*
[4]*Tokyo Institute of Technology, 2-12-1 Ookayama, Meguro-ku, Tokyo 152-8550 Japan*

[*]E-mail: yamazaki.yuichi@qst.go.jp

Received March 2, 2023; accepted March 13, 2023; published online March 27, 2023

Negatively charged boron vacancy (V_B^-) in hexagonal boron nitride has attracted attention as a promising spin defect for quantum sensing applications. Hence, a fabrication method for generation of V_B^- with superior spin properties would be desirable. In this study, we demonstrated V_B^- formation by two thermal treatment methods. Both methods improve the signal-to-noise ratio of optically detected magnetic resonance signal by a factor of 4. Furthermore, a zero-field splitting parameter E which reflects crystal distortion after irradiation significantly reduces for irradiation above 650 °C. These findings indicate that thermal treatment is an effective method for a V_B^- based quantum sensor.

Supplementary material for this article is available online

Quantum sensors using optically addressable spin defects in wide bandgap semiconductors, such as a negatively charged nitrogen-vacancy (NV^-) center in diamond[1–4] and negatively charged silicon vacancy (V_{Si}^-)[5–7] and NV^- centers[8,9] in silicon carbide (SiC), can measure magnetic and electric fields as well as temperature with high sensitivity and high spatial resolution. Therefore, these quantum sensors are expected to be used in a wide range of applications such as biosensors and various other electronic devices.[10–12] In sensing applications, the distance between the sensor probe and the measurement target must be as small as possible to enhance the sensitivity. However, in the case of three-dimensional (3D) materials, a spin defect near the surface does not function as a sensor because its charge state is changed due to band bending.[13] For this reason, it is difficult to reduce the distance to the measurement target when using 3D materials.

In contrast to 3D materials, two-dimensional (2D) materials are only composed of a single atomic layer, and therefore band bending is inherently unlikely to occur in these materials. Therefore, the distance to the measurement target can be shortened up to van der Waals radius, which enables very high sensitivity. Recently, spin defects have been found in hexagonal boron nitride (hBN),[14–16] a wide bandgap ($E_g \sim 6$ eV) semiconductor.[17] Among them, negatively charged boron vacancy (V_B^-)[18–23] is a single vacancy which can be formed without a post thermal treatment after energetic particle irradiation. Unlike other spin defects in 2D/3D materials, V_B^- defect shows a considerably large zero-field splitting (ZFS) parameter E in the spin Hamiltonian[24,25] which reflects crystal distortion around the V_B^-. This may be caused by a reduction in the crystalline quality of the hBN film due to energetic particle irradiation. Guo et al. reported that heavier ion irradiation led to a larger E based on optically detected magnetic resonance (ODMR) measurements.[25] Not only does the reduction of crystalline quality reduce the ODMR signal contrast but it also effects other spin properties such as spin–spin relaxation time T_2 as well.

We previously reported that thermal treatment can improve the ODMR signal contrast for V_{Si} in SiC because of the removal of unwanted defects.[26] The thermal stabilities of V_{Si} and unwanted defects were important factors for establishing the optimal thermal treatment condition to enhance the ODMR signal contrast. Furthermore, thermal treatment during irradiation may have a positive effect on the formation of desired defects since electron irradiation at high temperatures improves the creation efficiency of NV centers in diamonds.[27] Therefore, we are led to believe that thermal treatment during irradiation will act as a useful method to obtain V_B^- with high optical and spin properties. However, at present, the formation of V_B^- has only been carried out at room temperature, and the effect of thermal treatment on V_B^- fundamental properties such as its thermal stability has not been that well explored.

In this study, we investigated the effect of thermal treatment on V_B^- formation. Two thermal treatment methods, "high temperature irradiation" and "room temperature irradiation with subsequent annealing treatments (post irradiation annealing)," were demonstrated. Both treatments improve optical and spin properties of V_B^-. The improvements should be effective even for V_B^- in a thin hBN which is utilized for quantum sensors because they are caused by the processes involving the generation and annihilation process of defects including V_B^- and other defects.

Here we used high-temperature and high-pressure synthetic hBN crystal as a host material for V_B^- formation.[28] Samples were exfoliated hBN flakes placed on a Si substrate with 95 nm oxide layer. The thickness of the hBN flakes were 100 nm or more. Since V_B defects were formed within 100 nm of the surface of the hBN sample (See SRIM simulation result in Fig. S1), it is not necessary to consider differences in hBN film thickness in this study. High temperature ion irradiation was performed at temperatures ranging from 200 °C to 800 °C for 6 min whilst post irradiation annealing was performed at temperatures up to 600 °C for 6 and 30 min after ion irradiation at room temperature. N_2 ions with ion energy of 40 keV were

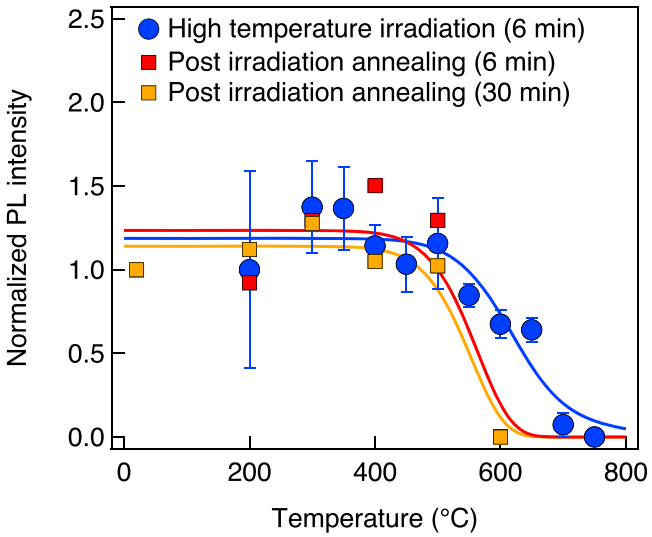

Fig. 1. (Color online) Temperature dependence of PL intensity for high temperature irradiation (blue circles) and post irradiation annealing (annealing time 6 min: red squares, 30 min: orange squares) obtained by integrating the PL spectra in Fig. S3. For high temperature irradiation, the average values of the data measured from 3 to 7 samples at each temperature are plotted, and the error bars are standard deviations. For post irradiation annealing, no error bars are shown because one sample is annealed repeatedly. The solid lines represent the theoretical curves obtained by the fitting where the high-temperature irradiation and post-annealing data were each fitted by Eq. (2) to derive the parameters including E_a with the summed smallest error for all fittings.

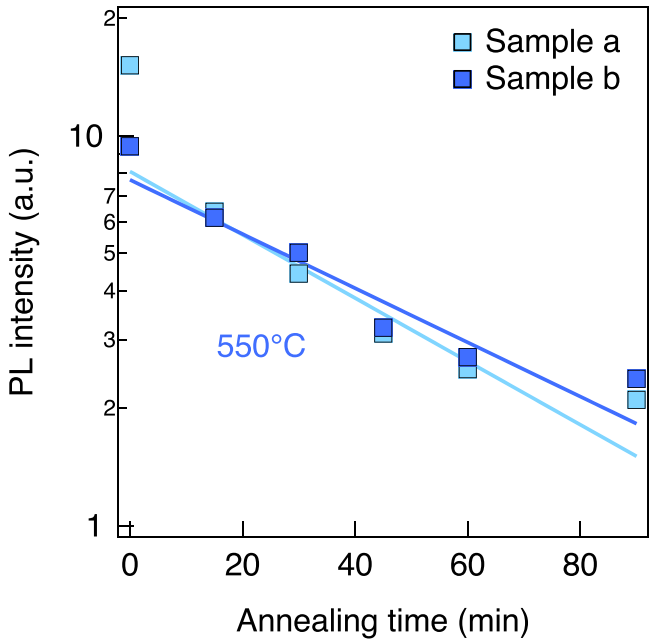

Fig. 2. (Color online) Dependence of PL intensity on annealing time (annealing temperature 550 °C) obtained by integrating the PL spectra in Fig. S4. The solid lines represent the theoretical values fitted using Eq. (2). The activation energy E_a used was the same value obtained from those in the temperature dependence measurements (Fig. 1).

irradiated at a fluence of 1×10^{15} cm^{-2}. Both ion irradiation and annealing were performed in vacuum. The quality of V_B^- formation was evaluated by photoluminescence (PL) and ODMR measurements. PL measurements were performed using a commercial confocal Raman microscope (HORIBA LabRAM HR Evolution). A home-made confocal microscope with 532 nm excitation laser was used for ODMR measurements. Photoemission from V_B^- was detected by an avalanche photodiode after filtering the signal using a 700 nm long-pass-filter. The photoemission signal generated by each sample was processed using a software lock-in system with AM modulated microwaves. Microwaves were applied to the sample through a 50 μm diameter copper wire. All measurements were carried out at room temperature in this study.

Firstly, we investigated the thermal stability of V_B^-. Figure 1 shows the dependence of PL intensity on irradiation temperature of the high temperature irradiation (blue circles) and that on annealing temperature of the post irradiation annealing (red squares: 6 min, orange squares: 30 min) calculated from PL spectra (shown in Fig. S3). In the case of high temperature irradiation, the PL intensity was almost constant below 500 °C and began to decrease with increasing temperature from 550 °C to 700 °C. No significant PL signal was observed above 750 °C. On the other hand, in the case of post irradiation annealing, PL was observed up to 500 °C and disappeared completely for samples post annealed at 600 °C. These results show that there is a difference of more than 100 °C in V_B^- residual temperature between high temperature irradiation and post irradiation annealing under our experimental conditions. This difference can be attributed to the fact that V_B^- formation and annihilation proceed simultaneously in the case of high temperature irradiation, but each formation or annihilation event proceeds individually in the case of post irradiation annealing. Thus the creation of V_B^- occurs consecutively during irradiation at elevated temperatures, and some amount of V_B^- remains at such high temperatures. To obtain the activation energy of V_B^- annihilation, we used the following differential equation

$$\frac{dN}{dt} = a - bN, (b = b'e^{-\frac{E_a}{kT}}), \quad (1)$$

where N is the number of V_B^-, a is the formation rate of V_B^- by ion irradiation, and b is the annihilation rate of V_B^- which is expressed by the Arrhenius equation (E_a is the activation energy of V_B^- annihilation, k is Boltzmann constant and T is absolute temperature). The first term indicates that the formation rate of V_B^- is constant since samples were irradiated with constant N_2 ion beam current. By solving Eq. (1), we obtain the number of V_B^-:

$$N = \frac{a}{b} + \left(N_0 - \frac{a}{b}\right)e^{-bt}, \quad (2)$$

where N_0 is the initial value of N and t is treatment time. Assuming that N is proportional to the PL intensity, the value of E_a was found to be 1.2 ± 0.4 eV from curve fitting the data shown in Fig. 1. Figure 2 shows the dependence of PL intensity on annealing time (annealing temperature = 550 °C) for samples prepared by room temperature ion irradiation calculated from PL spectra (shown in Fig. S4). PL intensity decreased exponentially with annealing time and was well fitted with the same E_a. Thus, Eq. (2) accounts for the effect of heat on V_B^- formation for both high temperature irradiation and post irradiation annealing. For high temperature irradiation, V_B^- created during the last few minutes of irradiation does not have enough time for annihilation to occur because the temperature is rapidly reduced to room temperature following the completion of the irradiation procedure. Thus, some amount of V_B^- remains using this

irradiation method. This leads to a smaller bN in Eq. (1), resulting in a difference of more than 100 °C in V_B^- residual temperature.

Next, we will discuss the annihilation process of V_B on the basis of its activation energy of $E_a = 1.2 \pm 0.4$ eV. Possible V_B annihilation processes and their activation energies based on theoretical studies[29,30] are shown below

1. $V_B + V_N \rightarrow V_B V_N$ ($E_a = 2.6$ eV)
2. $V_B + B_{knock\text{-}on}$
3. $V_B + N_{knock\text{-}on} \rightarrow N_B$.

Since the migration energy for V_B is 2.6 eV[29] and V_N defects are immobile below the melting point of hBN, process 1 can be ruled out. Process 2 (3) means that a knocked-on B (N) atom [denoted by $B_{knock\text{-}on}$ ($N_{knock\text{-}on}$)] occupies a boron substitution site. Weston et al. revealed that antisite defects have high formation energies,[30] indicating that process 3 is unlikely to occur in our experiments. The migration energy for an interstitial B atom (B_i) was calculated to be 0.5–1.1 eV depending on its charge state.[30] Since $B_{knock\text{-}on}$ can be considered to be a B_i, we estimated the activation energy to be 1.2 ± 0.4 eV which is consistent with the migration energy for $B_{knock\text{-}on}$. As for processes involving impurities, $V_B C_N$[15] is a possible product candidate for V_B annihilation because carbon is a major impurity in the hBN flakes used. The origin of the PL signal in 500–700 nm may be assigned to $V_B C_N$. However, the signal intensity changed little before and after post annealing (Fig. S3). Consequently, the main process of V_B annihilation is the incorporating of a $B_{knock\text{-}on}$ with a V_B (process 2).

In the following, we discuss the effects of high temperature irradiation and post irradiation annealing on parameters related to ODMR spectra. The ODMR signal contrast as a function of treatment temperature is shown in Fig. 3(a) (representative ODMR spectra are shown in insets). For high temperature irradiation, the improvement of ODMR contrast was saturated at 500 °C–650 °C. For post irradiation annealing, the contrast was maximized at 500 °C. This suggests that both thermal treatments above 500 °C are effective for removing unwanted defects whilst still producing a sufficient amount of V_B^-. A similar phenomenon was also observed for V_{Si} in SiC.[26] There was no significant change in the peak-width (FWHM) of any of the ODMR spectra (see Fig. S5 in supplementary material). Figure 3(b) shows the normalized ODMR signal-to-noise ratio (SNR) as a function of treatment temperature. The maximum absolute slope from the ODMR spectra divided by the product of standard deviation of signal intensity and square root of measurement time is defined as SNR. SNR showed almost the same trend as ODMR contrast. Both methods improve the SNR of ODMR signal by a factor of 4. This indicates that thermal treatment above 500 °C is an effective method to improve the sensitivity of V_B^- based quantum sensor.

Figure 4 shows the treatment temperature dependence of parameters E used to describe the ZFS of the triplet ground state in V_B^-. E showed the values ranging from 60–75 MHz, which are equivalent to previous studies,[25] below 600 °C for both high temperature irradiation and post irradiation annealing. For high temperature irradiation, E started to decrease above 650 °C. The value of E was found to be improved to as low as 44.8 MHz by irradiation at 700 °C. Since a smaller E corresponds to better crystalline quality, we concluded that high temperature irradiation is an effective process in forming V_B^- in hBN films whilst maintaining good crystallinity. The smaller E may improve spin properties of V_B^- such as T_2^*.

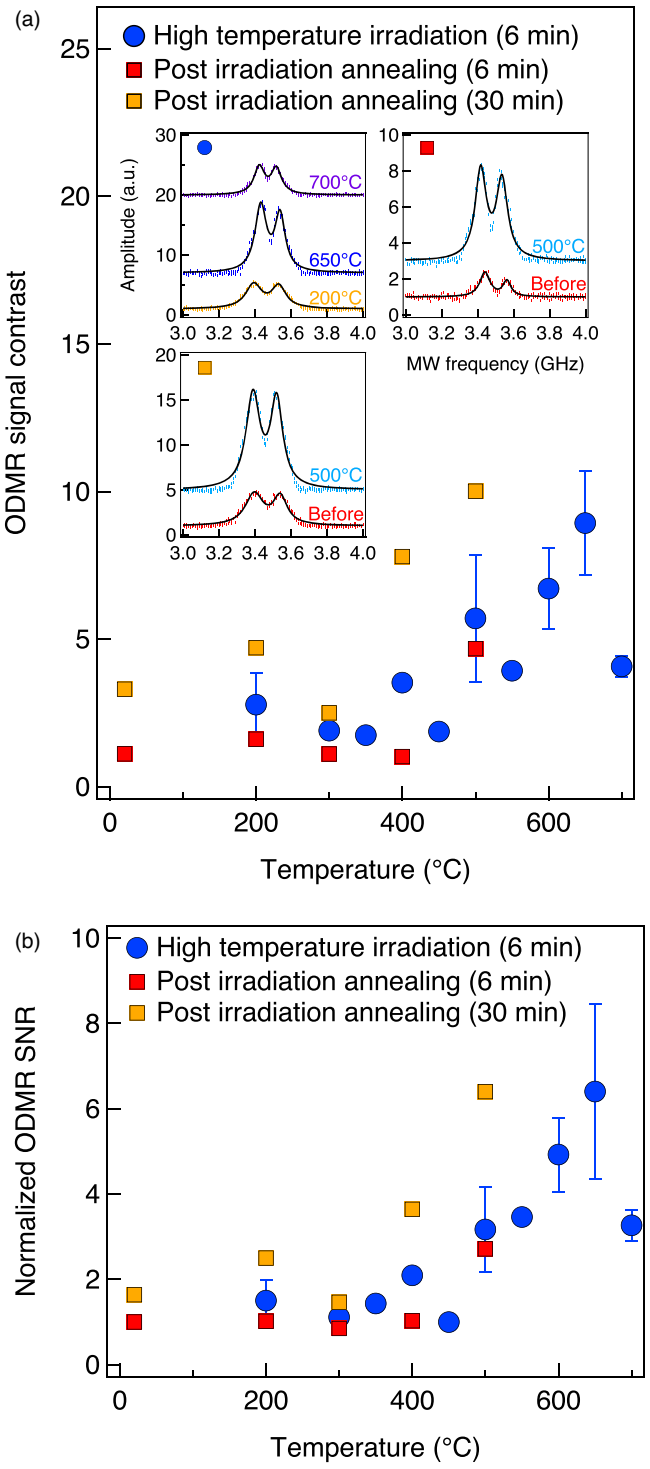

Fig. 3. (Color online) (a) Temperature dependence of the ODMR signal contrast. For high temperature irradiation, the contrast was saturated at 500 °C–650 °C. For post irradiation annealing, the contrast was maximized at 500 °C. Representative ODMR spectra are shown in insets. Each signal was processed using a software lock-in system. (b) The normalized ODMR signal-to-noise ratio (SNR) as a function of treatment temperature. The maximum absolute slope from the ODMR spectra divided by the product of standard deviation of signal intensity and square root of measurement time is defined as SNR. All data were normalized with respect to the initial value of post irradiation annealing (6 min).

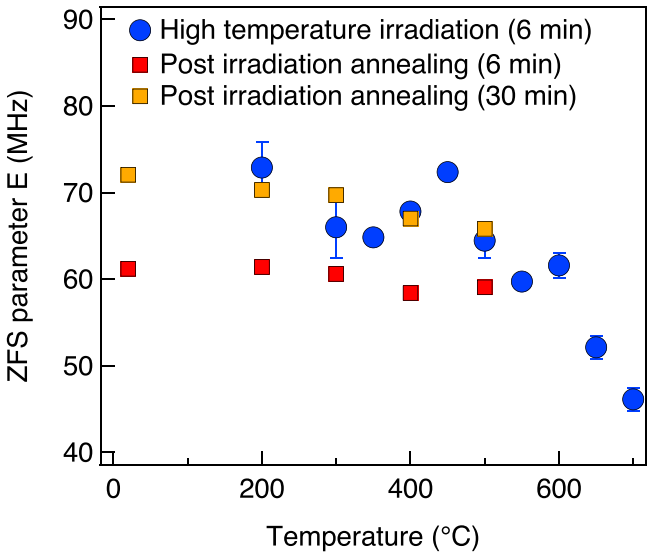

Fig. 4. (Color online) Temperature dependence of the ZFS parameter E. High temperature irradiation at 700 °C leads to the smallest E value.

In conclusion, we investigated the thermal stability of V_B^- and the effect of thermal treatments on V_B^- formation and their spin properties. We demonstrated two fabrication methods to generate V_B^-, high temperature irradiation and post irradiation annealing. The former can generate V_B^- at more than 100 °C higher temperature than the latter. Based on the analysis using our generation-annihilation model, we obtained the activation energy for V_B^- annihilation of 1.2 ± 0.4 eV. We suggest that the reason why high temperature irradiation can generate V_B^- at a higher temperature is that unlike in the case of post irradiation annealing, the formation and annihilation of V_B^- occur simultaneously during high temperature irradiation. This implies that there is room for further optimization of the formation of V_B^- with higher optical and spin properties in future. We conclude that the process of V_B annihilation was attributed to the coupling of V_B and $B_{knock\text{-}on}$. ODMR signal contrast reached a maximum value at 500 °C and 500 °C–650 °C for post irradiation annealing and high temperature irradiation, respectively. Both methods improve the SNR of ODMR signal by a factor of 4. In addition, high temperature irradiation treatment at 700 °C leads to the smallest ZFS parameter E. The findings in this study suggest that high temperature irradiation is an effective method to form V_B^- centers in hBN films whilst maintaining good crystalline quality. These findings indicate that thermal treatment is an effective method to fabricate V_B^- centers for quantum sensor applications.

This research has been supported by the QST President's Strategic Grant QST Creative Research and JSPS KAKENHI No. 20K05352.

ORCID iDs Takeshi Ohshima https://orcid.org/0000-0002-7850-3164

1) J. R. Maze et al., Nature **455**, 644 (2008).
2) G. Balasubramanian et al., Nature **455**, 648 (2008).
3) F. Dolde et al., Nat. Phys. **7**, 459 (2011).
4) P. Neumann et al., Nano Lett. **13**, 2738 (2013).
5) H. Kraus, V. A. Soltamov, F. Fuchs, D. Simin, A. Sperlich, P. G. Baranov, G. V. Astakhov, and V. Dyakonov, Sci. Rep. **4**, 5303 (2014).
6) F. Fuchs, B. Stender, M. Trupke, D. Simin, J. Pflaum, V. Dyakonov, and G. V. Astakhov, Nat. Commun. **6**, 7578 (2015).
7) T. M. Hoang, H. Ishiwata, Y. Masuyama, Y. Yamazaki, K. Kojima, S.-Y. Lee, T. Ohshima, T. Iwasaki, D. Hisamoto, and M. Hatano, Appl. Phys. Lett. **118**, 044001 (2021).
8) J.-F. Wang et al., Phys. Rev. Lett. **124**, 223601 (2020).
9) Z. Mu et al., Nano Lett. **20**, 6142 (2020).
10) R. Schirhagl, K. Chang, M. Loretz, and C. L. Degen, Annu. Rev. Phys. Chem. **65**, 83 (2014).
11) S. Sotoma, C. P. Epperla, and H.-C. Chang, Chem. Nano Mater. **2**, 15 (2018).
12) T. Ohshima, T. Satoh, H. Kraus, G. V. Astakhov, V. Dyakonov, and P. G. Baranov, Appl. Phys. **51**, 333002 (2018).
13) B. K. Ofori-Okai, S. Pezzagna, K. Chang, M. Loretz, R. Schirhagl, Y. Tao, B. A. Moores, K. Groot-Berning, J. Meijer, and C. L. Degen, Phys. Rev. B **86**, 081406 (2012).
14) A. Gottscholl et al., Nat. Mater. **19**, 540 (2020).
15) N. Mendelson et al., Nat. Mater. **20**, 321 (2021).
16) N. Chejanovsky et al., Nat. Mater. **20**, 1079 (2021).
17) G. Cassabois, P. Valvin, and B. Gil, Nat. Photon. **10**, 262 (2016).
18) M. Kianinia, S. White, J. E. Fröch, C. Bradac, and I. Aharonovich, ACS Photon. **7**, 2147 (2020).
19) V. Ivády, G. Barcza, G. Thiering, S. Li, H. Hamdi, J. Chou, Ö. Legeza, and A. Gali, npj Comput. Mater **6**, 41 (2020).
20) A. Gottscholl, M. Diez, V. Soltamov, C. Kasper, A. Sperlich, M. Kianinia, C. Bradac, I. Aharonovich, and V. Dyakonov, Sci. Adv. **7**, 14 (2021).
21) A. Gottscholl, M. Diez, V. Soltamov, C. Kasper, D. Krauße, A. Sperlich, M. Kianinia, C. Bradac, I. Aharonovich, and V. Dyakonov, Nat. Commun. **12**, 4480 (2021).
22) X. Gao et al., Nano Lett. **21**, 7708 (2021).
23) W. Liu et al., Nat. Commun. **13**, 5713 (2022).
24) W. Liu et al., ACS Photon. **8**, 1889 (2021).
25) N.-J. Guo et al., ACS Omega **7**, 1733 (2022).
26) Y. Chiba, Y. Yamazaki, S. I. Sato, T. Makino, N. Yamada, T. Satoh, Y. Hijikata, and T. Ohshima, Sci. Forum **1004**, 337 (2020).
27) M. Capelli, A. H. Heffernan, T. Ohshima, H. Abe, J. Jeske, A. Hope, A. D. Greentree, P. Reineck, and B. C. Gibson, Carbon **143**, 714 (2019).
28) T. Taniguchi and K. Watanabe, J. Cryst. Growth **303**, 525 (2007).
29) A. Zobelli, C. P. Ewels, A. Gloter, and G. Seifert, Phys. Rev. B **75**, 094104 (2007).
30) L. Weston, D. Wickramaratne, M. Mackoit, A. Alkauskas, and C. G. Van de Walle, Phys. Rev. B **97**, 214104 (2018).